

Material Behaviour at High Strain Rates*

L. W. Meyer

Chair Materials and Impact Engineering, Chemnitz University of Technology, Germany

Abstract

An overview is given of high rate mechanical testing procedures and the material behaviour under tensile, compression, and shear loading as well as under biaxial loading states tension/compression with torsion resp. shear.

Keywords:

Material, Strain rate, Behaviour

1 Introduction

For the characterisation of deformation processes of metallic materials the knowledge of flow and failure plays an essential role. But flow and failure are not independent material properties, they are influenced strongly by stress state, temperature and strain rate. Due to microstructural reasons combined with dislocation mechanics, the flow stresses, deformability, or toughness changes with strain rate. Most technical production methods like cutting, forging, stamping, or forming reach strain rates up to 10^2 to 10^4 s⁻¹ which cover or overlap the high energy rate fabrication HERF-procedures. This gives reason and a strong need to explore the high rate material behaviour, because not only the strength, but the deformability is changed, too. The former named velocity embrittlement has disappeared nearly completely due to modern material production methods. Contrarily, the fracture strain of bcc - steels often is enhanced by 20 to 50% at strain rates at about $\dot{\epsilon} = 10^3$ s⁻¹ [1]. The reasons are not fully understood, but twinning and adiabatic heating may play a role [2]. These differences to the quasistatic deformability are determined without any doubts, because the elongations are measured after the tests with arbitrary precision. The problems of force or stress measurement at higher strain rates arise when the weight of the load cell (adapted to the load capability of the testing machine) and the corresponding stiffness are leading to eigenfrequencies of some kHz or ringing periods of

*This work is based on the results of DFG and BMVg-public research; the author likes to thank for their financial support and interest

milliseconds or shorter. Only when the complete mechanical and electrical force measuring circuit exhibits bandwidths of 10 x more than the frequency response of the testing procedure contains, the basic requirements of measurement rules are fulfilled. This is easy and self-evident to demand, but not easy to fulfil. All known hydraulic driven testing machines are much quicker with the piston velocity than the load cell is able to follow. In a tensile test of a universal testing machine a third of the maximum piston velocity of $v_{\max} = 0.5$ m/s with $v = 0.15$ m/s is used, Figure 1, and the original force-time-record, trace a), presents as expected yielding, strain hardening, maximum, reduction of area, and fracture, of course with some ringing. When this ringing of 400 kHz is smoothed out, and it is often claimed that this is allowed, then the following trace is found, trace b). In the same test another load cell with a higher eigenfrequency of 65 kHz was used, trace c), which is not affected or animated by the frequency spectrum of the testing event.

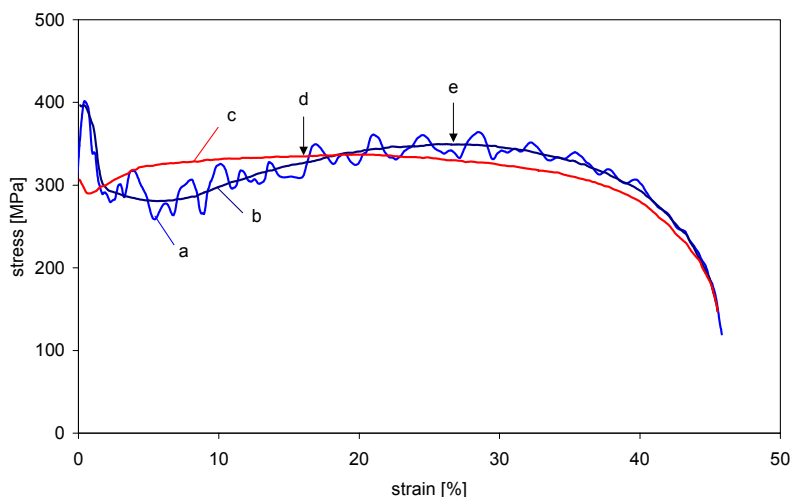


Figure 1: Stress-strain traces of a tensile test in a hydraulic Universal testing machine with 150 mm/s piston velocity (max. possible is 500 mm/s) a) virgin stress trace of the original load cell; b) smoothed stress trace of the original load cell; c) stress trace of separate high eigenfrequency load cell; d) UTS and $\epsilon_{\text{uniform}}$ with high bandwidth; e) UTS and $\epsilon_{\text{uniform}}$ with original bandwidth

The difference in strain hardening and homogenous strain determination is obvious. The reason for the deviations is that the observed frequency is not the base mode, but the second mode. The first mode is covered by the low fracture strain resp. the short testing time. If a longer specimen with a higher elongation would have to be used, than the first mode of ringing would appear with several full periods and not less than one, as shown here. The same principle is existing at higher strain rates. Therefore, for a satisfying reliability the original traces should be presentable.

2 Testing Procedures

2.1 Tensile Testing

To study the flow behaviour with strain rates above $\dot{\epsilon} > 1 \text{ s}^{-1}$, the specimen are instrumented with strain gages in the gage length and on a cone with 8° just aside the

gage length, Figure 2. With $l/d = 3$ and $d = 3,56$ mm resp. a cross section of $A = 10$ mm² strain rates up to $\dot{\epsilon} = 10^3$ s⁻¹ can be used without the necessity of curve smoothing.

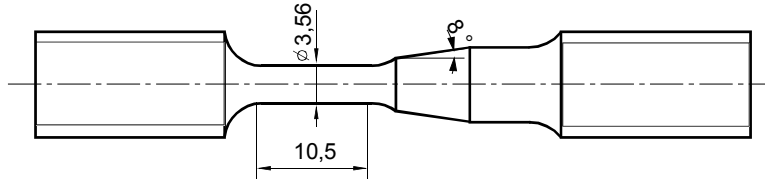


Figure 2: Tensile specimen, optimised for high rate testing with $l/d = 3$, $d = 3.56$ mm, cone 8° , gages at cone and in the gage length

With warm aging adhesives, the strain gages are usable to more than 6% plastic strain. With the known Young's modulus, the elastic strains at the cone are converted into stresses acting at the gage length. With recognising the wave speed and distance of less than 10 mm between gage length and gage area at the cone, a determination of the Young's modulus is possible in each test. This is a valuable control of the alignment of the specimen and the electronic set up. The high rate tensile deformation can be done by fast hydraulic, hopkinson, or rotating wheel devices set ups [3,4]. A careful alignment is necessary in each case. Because of wave reflections between specimen and hopkinson bars above $\dot{\epsilon} = 10^3$ s⁻¹, several methods of replacing the threads were tested, like e.g. brazing, gluing and, welding. The best results are reached with friction welding, which avoids differences of the acoustic impedance. The material to be tested is friction welded onto a 2 m long hopkinson bar and machined afterwards, Figure 3.

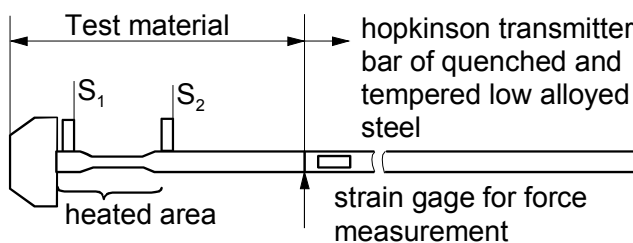


Figure 3: High temperature, high rate tensile testing with direct hopkinson bar set up (DHB) S_1 , S_2 = marker for touchless displacement measurement

This procedure can lead to undisturbed records between $\dot{\epsilon} = 10^3$ and 10^4 s⁻¹ and is, to our knowledge, the only way to reach clear results. Of course, strain rates of about 10^4 s⁻¹ or 1% strain per microsecond force to use short, small specimen of 0.5 to 2 mm gage length and even then no $R_{p0.2}$, but only R_{p2} and higher can be determined accurately, because of the limited plastic wave speed and the requirement of stress balance along the length of the specimen. With the short specimen, the attachment of strain gages at the gage length becomes difficult or impossible. Instead, an electro-optical displacement transducer of Zimmer Ltd. gives a solution. The same procedure is needed for high rate, high temperature testing, e.g. of turbine blades, containment materials, or explosions of steam tubes, Figure 4, where for temperature reasons strain gages cannot be used. The left Figure 4 of the behaviour of a quenched and tempered steel presents a smooth transition between elastic and plastic elongation and nearly no ringing at $\dot{\epsilon} = 10^3$ s⁻¹. The right side Figure 4 of stress-time-curves of a 0.45% carbon-steel presents in an excellent manner

the high ability of this testing method of recording undisturbed measurements, even when a pronounced upper and lower yield stress by interstitials gives best conditions for initiating mechanical ringing. Such a material behaviour is exacting highest claims to the fidelity of the stress measurement.

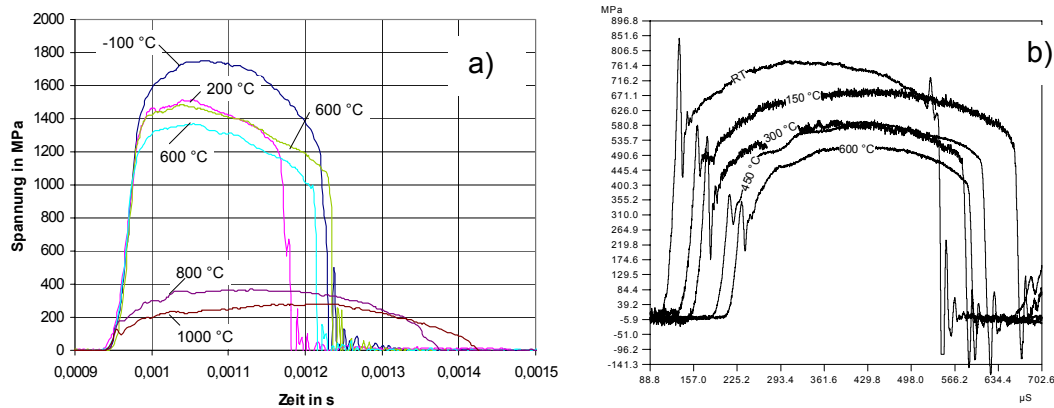


Figure 4: Tensile results at $\dot{\epsilon} = 10^3 \text{ s}^{-1}$ at room and elevated temperature of quenched and tempered steel, b) 0.45% carbon steel

2.2 Testing Compression

Tensile testing of the amount at homogenous strain limits the flow curve to $0.05 < \varphi < 0.2$. Under compression, higher true strains are reachable until friction problems transfer the uniaxial stress state into a multiaxial one. Good lubrication and control are essential [5]. With a drop weight principle, high energies are available with strain rates between 10^2 and $5 \cdot 10^2 \text{ s}^{-1}$. The high energy ensures nearly a constant striking velocity up to the desired deformation, stopped by blocking.

Split hopkinson pressure bars (SHPB) are common, well understood [6]. The main advantage is the simple mechanical and electronic set up. Surely, for very high strain rates at 10^4 s^{-1} again the specimen length has to be reduced to about 1 mm or less, which leads to the necessity of small diameters of the bars and the avoiding of buckling of the bar.

After regrinding the front surface of a meanwhile penny shaped deformed compression specimen and reheating, further compression deformation up to $\varphi = 1.5$ is possible under controlled friction conditions. These investigations revealed that the steady state of recrystallisation, which is known from high temperature medium velocity forging [7], is present, too, at low temperature high rate compression conditions, Figure 5.

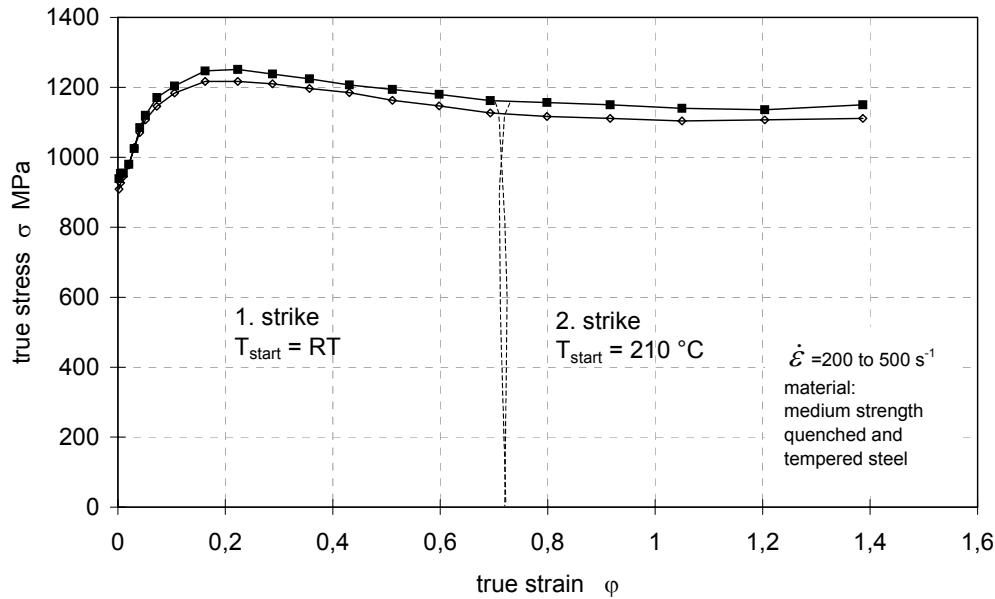


Figure 5: Flow curve under compression loading, 2nd strike with two specimen as a block with enhanced starting temperature

Such a behaviour is not easy to be described by constitutive equations of the Johnson-Cook-type, because the steady state ($\sigma = \text{const}$) is not considered.

The dropweight towers have further advantages with high rate bending or fracture toughness, both without ringing. A valuable testing possibility is the biaxial compression with shear component testing, figure 6.

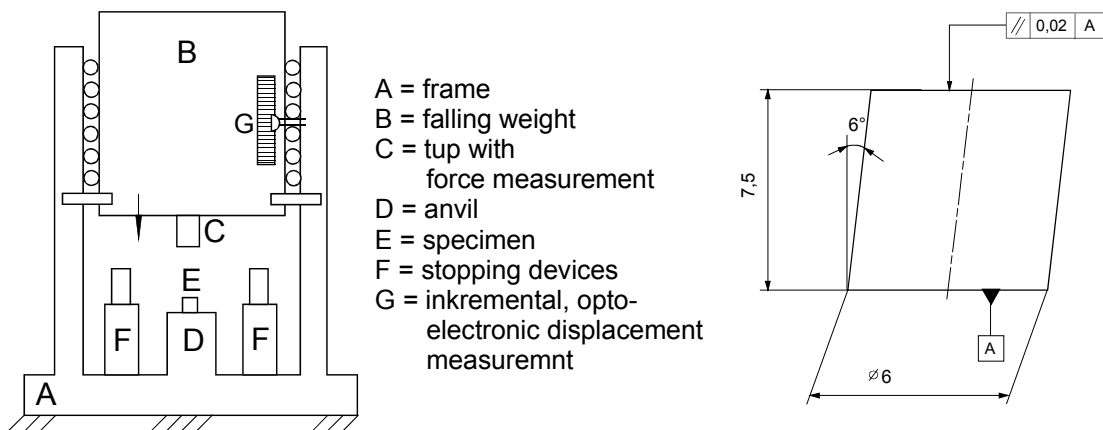


Figure 6: Principle of drop weight machine with biaxial compression/shear specimen with $h/d = 1.25$, front faces need to be parallel to 0.01 mm

Under pure compression, only a few materials like high strength steels or titanium alloys fail due to a adiabatic shear failure [8], Figure 7. With the aid of a few percent added shear stresses resp. with the transition to a slight biaxial stress state, many medium strength materials decide to fail under adiabatic conditions, too, Figure 8 [9].

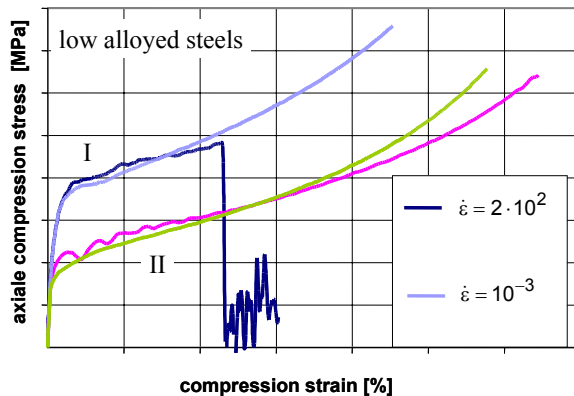


Figure 7: Influence of hardness (I and II) and strain rate (10^{-3} and 10^2 s^{-1}) on deformability

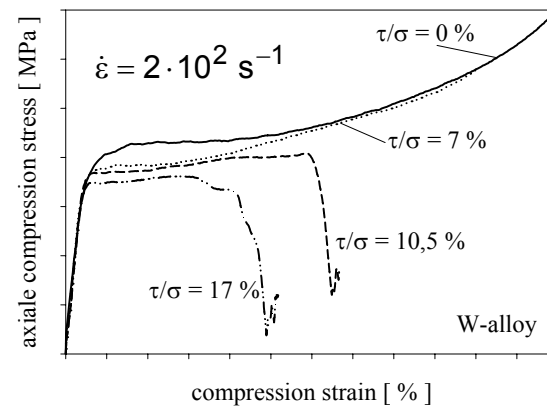


Figure 8: Influence of biaxial loading at $\dot{\epsilon} = 2 \cdot 10^2$ s^{-1} of W-alloy on deformability

With using the “hat shaped” specimen [1], the material is forced to shear under adiabatic conditions, even when it is not prone to it [10]. The constraint character of the hat shaped specimen was changed into an “offer” of a biaxial stress state and the material is answering with different behaviour or failure occurrence: early, late, or not at all. This new compression-shear testing, Figure 6, as well as the hat shaped testing was accepted by the American Society of Metals and is included in the new handbook No. 8, 10th ed. [11], serving as a recommendation for a standard testing procedure.

2.3 Torsion testing

The industrial forming, not only the high rate forming often applies compression and shear loading states. This is due to the non activation or suppressing of tensile cracks. To explore the behaviour under this loading state, shear testing is needed. Nevertheless, generating exact shear or torsion loading states without additional bending is a difficult task. Therefore, hydraulic torsion machines or hopkinson torsion bars are not common. Stiebler created a modified tension-Torsion hopkinson set up [12]. In all cases the torsion angle is limited by the strength and length of specimen and bars. To reach, especially under torsion, the material limit of high shear straining at strain rates of 10^3 s^{-1} and higher, as well as with enhanced temperatures above $1000^{\circ}C$, a new kind of torsion testing device was developed in Chemnitz, namely a modified direct torsion hopkinson machine, Figure 9.

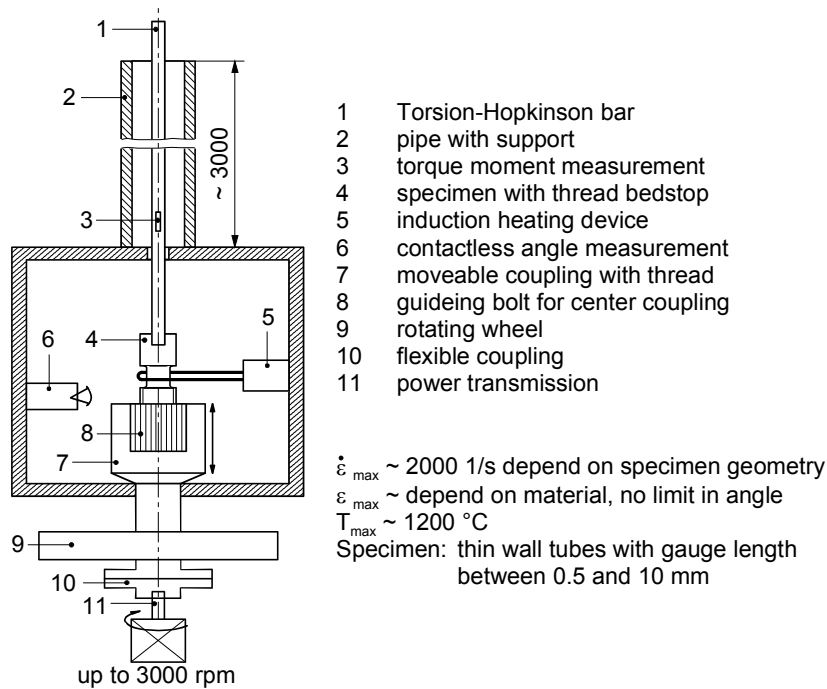


Figure 9: Principle of direct torsion hopkinson machine of LWM, Chemnitz University of Technology

With a strong motor of a machine-tool from a few to 3000 rpm with a torque of 300 Nm, all continuous cyclic or incremental strain paths up to unlimited revolutions are available with the same specimen geometry.

3 Material Behaviour

The flow stress behaviour can be divided into two or three regimes, the non-velocity-sensitive so-called athermal behaviour (temperature, but not rate dependant), the mutual influence of temperature and strain rate (thermal activated, “linear” in temperature, logarithmic with strain rate), and the dislocation drag regime with a linear influence of strain rate, expected at strain rates above 10^3 s^{-1} [13]. Aluminium and aluminium alloys behave mostly athermal. Low alloyed steels, too, are rate insensitive up to 10^{-1} s^{-1} . Mild steel, sheet metals, carbon steels, austenitic steels, even maraging steels, are rate sensitive between 30 to 120 MPa per order of magnitude in strain rate [14]. The compression behaviour, even from the same batch and without texture influence, mostly is enhanced, compared to the tensile behaviour [15], Figure 9.

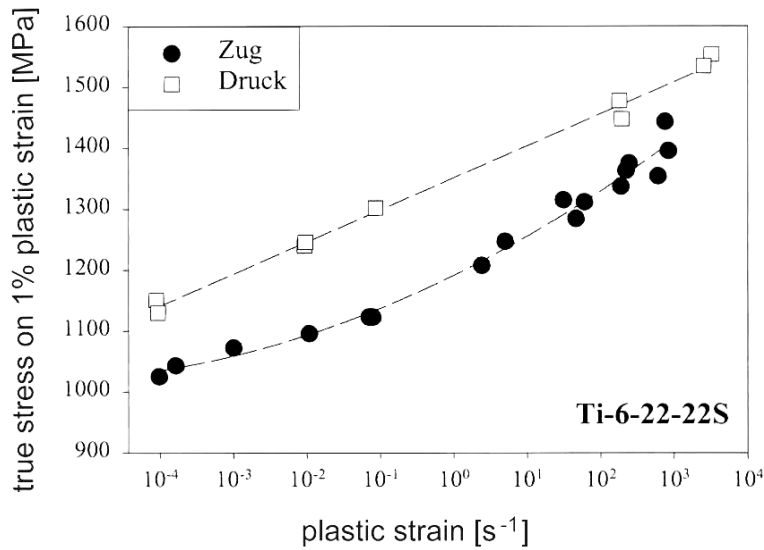


Figure 10: 1%-tensile yield stress and 1%-compression yield stress as a function of strain rate

This is named strength differential effect or SD-effect. It varies with strain rate and strain, differences up to 18% are known [16]. The same Ti-6-22-22S of figure 10 was tested under flyer data conditions to reach $\dot{\epsilon} = 10^5 \text{ s}^{-1}$. With the evaluation of uniaxial 0.2 – yield and 2% - flow stress of Kanel and Razorenov [17], a long missing connection between impact data and high rate uniaxial material properties is achieved. The result of Ti-6-22-22S indicates that the thermal activation rules the behaviour at low activation energies resp. at high strain rates up to 10^5 s^{-1} , Figure 11.

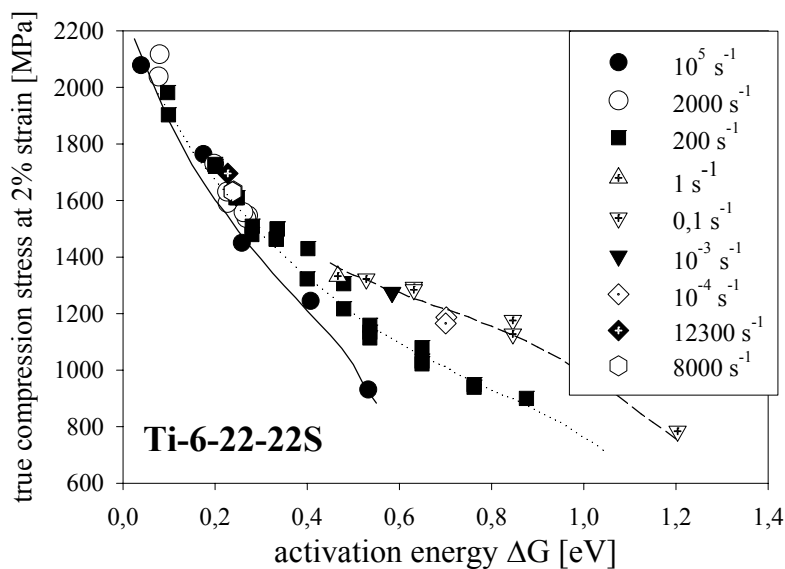


Figure 11: 2% true compression stress versus activation energy with temperature

This is true for other materials, too. In figure 12 the 0.2 – flow stress versus the strain rate of a high annealed tool steel 40CrMnMo7 is continuously increasing without any sharp increase beyond $\dot{\varepsilon} = 10^3$ and higher. There is no hint for a drag effect on the stress behaviour to be detected. The reasons for the detected stronger increase above $\dot{\varepsilon} = 10^3 \text{ s}^{-1}$ at other materials are still under discussion. Additional proofs are necessary.

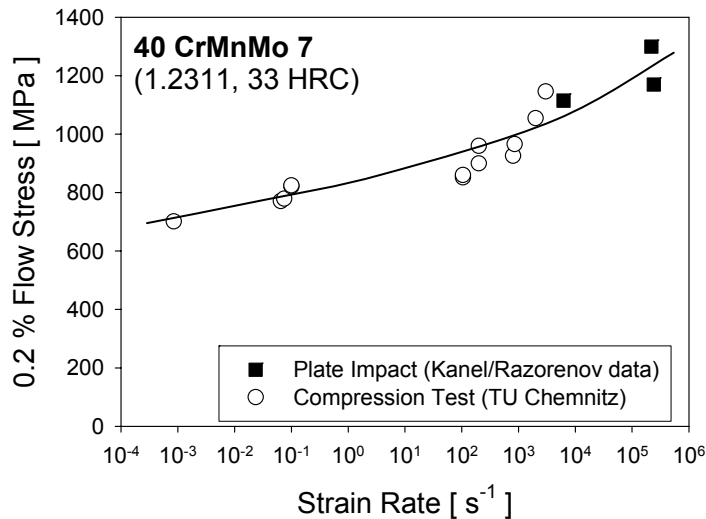


Figure 12: 0.2 yield stress versus strain rate $\dot{\varepsilon}$ from compression tests (4 \varnothing and 2 \varnothing mm specimen) and from plate impact test, conducted by Kanel and Razorenov from the same 1.2311 material

Under multiaxial loading the material flows, when a certain critical stress is exceeded. This stress, equivalent to a uniaxial stress, is defined by mostly two theories, Tresca and v. Mises. For a biaxial loading of a normal and a shear stress, the equivalent stress and strain is defined by

$$\sigma_{eq} = \sqrt{\sigma^2 + a \cdot \tau^2} \quad ; \quad \varepsilon_{eq} = \sqrt{\varepsilon_{ax}^2 + \frac{1}{a} \gamma^2} \quad (1)$$

with $a = 3$ for v. Mises's or $a = 4$ for Tresca's theory.

Often, the reality can be described best with the adapting parameter $a = 3.5$, which is just between both theories, here for a HY80 steel [18], Figure 13 and 14.

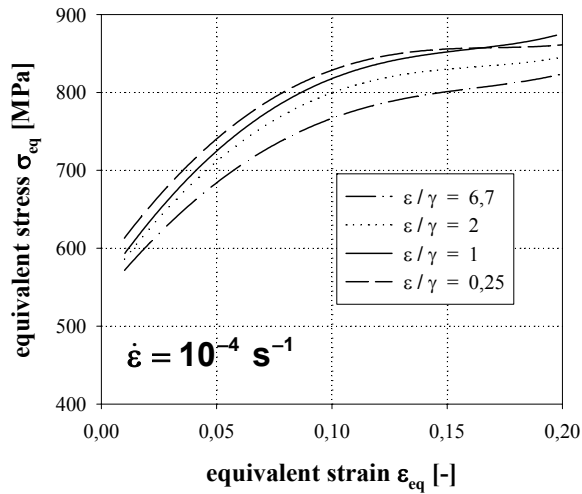


Figure 13: Equivalent stress – equivalent strain curves of steel HY80 using the v. Mises criterion ($a = 3$)

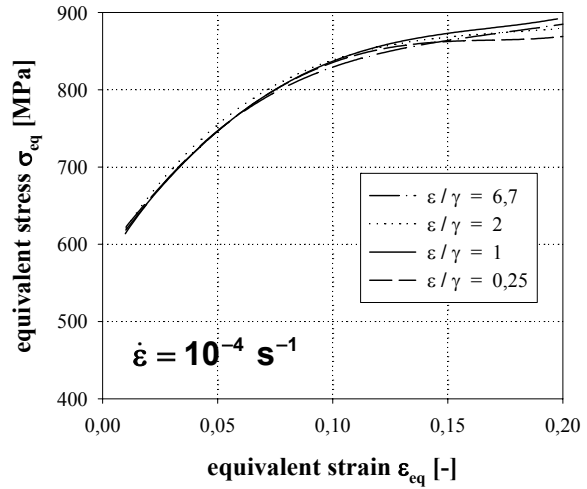


Figure 14: Equivalent stress – equivalent strain curves of steel HY80 using the adapting parameter ($a = 3.5$)

With increasing strain rate, a similar stress enhancement under the biaxial loading state takes place like under monoaxial loading, and the yield loci enlarge. In the first quadrant, the highest reached strain rate with a modified tension-torsion hopkinson bar yielded strain rates of $\dot{\epsilon}_{eq} = 300 - 400 \text{ s}^{-1}$. The form of the 1% - yield loci tends to narrow v. Mises behaviour. These results are valid for the low alloyed tool steel 40CrMnMo7 [19], Figure 15.

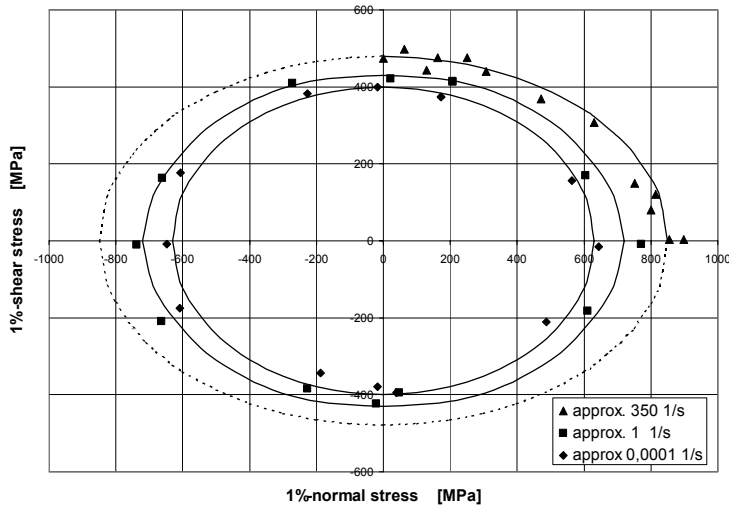


Figure 15: Yield surface of 1.2311 (40CrMnMo7), quenched and tempered at 650°C at low and high strain rates

4 Summary

The high rate material characterisation has made encouraging progress in the last decade, but further important tasks of e.g. dynamic multiaxial strength and failure behaviour in highspeed forming processes are waiting for deeper insight.

References

- [1] *Hartmann, K.-H.; Kunze, H.-D. Meyer, L.W.:* Metallurgical Effects on Impact Materials. in: Shock Waves and High Strain Rate Phenomena in Metals, Hrsg. M.A. Meyers and L.E. Murr, Plenum Press, New York 1981, S. 325-337.
- [2] *Reinders, B.-O.; Kunze, H.-D.:* Influence of Mechanical Twinning on the Deformation Behavior of Armco Iron. in: Shock Waves and High-Strain-Rate Phenomena in Materials Eds. M.A. Meyers, L.E. Murr, K.P. Staudhammer, M. Dekker, 1990, S. 127-136.
- [3] *Nemat-Nasser, S.:* High Strain Rate Tests. in: ASM Handbook No. 8, 10th ed., Mechanical Testing and Evaluations, ASM International 2000, Materials Park, Ohio, p. 425 – 475.
- [4] *Field, J.E.; Walley, S.M.; Bourne, N.K. and Huntley, J.M.:* Review of Experimental Techniques for High Rate Deformation Studies. Proc. Acoustics and Vibration Asia '98 (Singapore), 1998, p. 9-38.
- [5] *Gorham, D.A.; Pope, P.H. and Cox, O.:* Sources of Error in Very High Strain Rate Compression Tests. Inst. Phys. Conf. Series, Vol. 70, 1984, p.151-158.
- [6] *Gray III, G.T.:* Classic Split Hopkinson Pressure Bar Testing. Asm Handbook No. 8, Mechanical Testing and Evaluation, 10th ed. ASM International 2000, Materials Park, Ohio, USA, p. 462-476.
- [7] *Weise, A.:* Entwicklung von Gefüge und Eigenspannungen bei der thermischen Behandlung von Stahl. PhD-Thesis, Chemnitz University of Technology, 1988.
- [8] *Meyer, L.W.:* Dynamic Behaviour of Thermomechanically Treated Ultra High Strength Steel under Tensile and Compressive Loading. in: High Energy Rate Fabrication - 1984, Hrsg.: I. Berman and J. W. Schroeder, ASME, New York, S. 245-252.
- [9] *Meyer, L.W.; Staskewitsch, E. Burblies, A.:* Adiabatic Shear Failure under Biaxial Dynamic Compression/Shear Loading. in: Mechanics of Materials 17, 1994, S. 203-214.
- [10] *Hines, J.A. and Vecchio, K.S.:* Dynamic recrystallization in adiabatic shear bands in shock-loaded copper. Metallurgical and Material Applications of Shock-Wave and High-Strain-Rate Phenomena, eds. L.E. Murr, K.P. Staudhammer and M.A. Meyers, 1995, Elsevier Science B.V.
- [11] *Meyer, L.W. and Krüger, L.:* Drop Weight Compression Shear Testing. ASM Handbook No. 8, Mechanical Testing and Evaluation, 10th ed., ASM International 2000, S. 452-454.
- [12] *Stiebler, K.; Kunze, H.-D. and El-Magd, E.:* Description of the Flow Behaviour of a High Strength Austenitic Steel under Biaxial Loading by a Constitutive Equation. Nuclear Engineering and Design, Vol. 127, 1991.

- [13] *Campbell, J.D. and Ferguson, W.G.:* The Temperature and Strain Rate Dependence of Shear Strength of Mild Steel. *Philos. Mag.*, Vol. 21, 1970, p. 63-82.
- [14] *Kunze, H.-D.; Meyer, L.W.:* Materials for Extreme Dynamic Loads. in: *Metallurgical Applications of Shock Waves and High-Strain-Rate Phenomena*, Eds. L.E. Murr, K.P. Staudhammer, M.A. Meyers, Marcel Dekker, New York, Basel, 1986, S. 481-507.
- [15] *Krüger, L.:* Untersuchungen zum Festigkeits-, Verformungs- und Versagensverhalten der Legierung Ti-622-22S in Abhängigkeit von der Temperatur, der Dehngeschwindigkeit und dem Spannungszustand, Dissertation TU Chemnitz, Lehrstuhl Werkstoffe des Maschinenbaus, 2001.
- [16] *Meyer, L.W. and Abdel-Malek, S.:* Strain Rate Dependence of Strength-Differential Effect in Two Steels. in: *J. de Physic IV*, Vol. 10, 2000, p. 9-63.
- [17] *Meyer, L. W.; Krüger, L.; Razorenov, S. V.; Kanel, G. I.:* Investigation of dynamic flow and Strength properties of Ti-6-22-22S at normal and elevated temperatures in: *International Journal of Impact Engineering* 28 (2003) S. 877-890.
- [18] *Meyer, L.W. and Hahn, F.:* Dynamic Material Behaviour under Biaxial Loading. in: *Schock-Wave and High-Strain-Rate Phenomena*, eds. K. Staudhammer, L.E. Murr and M.A. Meyers, Elsevier, 2001, S. 11 – 24.
- [19] *Halle, T.:* Untersuchungen zum mechanischen Werkstoffverhalten der Stähle C45E und 40CrMnMo7 und Korrelation mit HSC Spanergebnissen. Dissertation TU Chemnitz, Lehrstuhl Werkstoffe des Maschinenbaus, planed in 2004.